Synthesis of Distributed Elliptic-Function Filters from Lumped-Constant Prototypes

R. LEVY, SENIOR MEMBER, IEEE, AND I. WHITELEY, STUDENT MEMBER, IEEE

Abstract—A synthesis procedure for distributed elliptic-function filters utilizing published tables of lumped-constant elliptic-function filters has been devised. It is dependent upon the application of a new generalized transformation for distributed networks. The filters often require the realization of distributed Brune sections, and several novel practical realizations are given both for general and degenerate Brune (i.e., Foster) sections. Examples are given of elliptic function stop band and pass band filters having both wide and narrow bandwidths, and experimental results show good agreement with theory.

I. Introduction

THE FILTERS described in this paper are based on the elliptic-function or Cauer-parameter lumped-element prototype [1], [2]. A typical insertion loss vs. frequency characteristic for a low-pass prototype is shown in Fig. 1, which represents a filter having two transmission zeros at finite frequencies, and one at $\omega=\infty$. The ripple level in the pass band is A_D dB, and the minimum stop band attenuation is A_S dB, where the pass band edge is normalized to $\omega=1$ and the stop band edge is at $\omega=\omega_s$. The main advantage of this type of characteristic is that the cutoff slope, which may be defined as

$$S_{\text{dB}} = \frac{A_S - A_D}{\omega_s - 1}, \tag{1}$$

may be made very large with a reasonably small number of circuit elements. This may be contrasted with Butterworth or Chebyshev filters, where very often a rather large number of circuit elements are required. A second advantage, of considerable practical importance, is that extensive design tables for elliptic-function filters are available [2].

Although elliptic-function filters have been developed and are employed extensively at low frequencies using lumped components, there has been little application of the technique in the microwave band, using distributed circuit elements. Ozaki and Ishii [3] made an early reference to a design procedure but their method consists of a direct synthesis from the network function, and appears to be quite complicated. An interesting procedure based on coupled transmission lines was introduced by Saito [4]. It is subject to limitations due to extreme impedance levels. A method (which also suffers from restrictions) similar to that described in Section VI of the present paper has been published independently by Blanc and Soldi [5], and a very compact design for broadband elliptic-function filters has been given by Horton and Wenzel [6]. A multiharmonic rejection filter designed from an elliptic-function prototype has been described by Schiffman [7], but is limited to prototypes having not more than one transmission zero at a finite frequency. A more empirical approach to obtaining high rates of cutoff at the band edges has also been described by Torgow and Lubell [8].

Although direct synthesis of distributed elliptic-function filters is certainly possible [3], a great deal of work is involved in the preparation of suitable computer programs. As an alternative it was decided to take advantage of the considerable effort which has led to the publication of comprehensive tables for lumped-element elliptic-function filters [2]. The distributed filters described in this paper use the low-pass prototypes of these tables.

Manuscript received December 27, 1965; revised August 2, 1966. This work was supported by the Ministry of Aviation under Contract PD/62/022. The work of I. Whiteley was supported by a maintenance grant from the Science Research Council.

The authors are with the Department of Electrical and Electronic Engineering, The University of Leeds, Yorkshire, England.

II. Lumped to Distributed Transformations

The extension of network synthesis to distributed networks was demonstrated by P. I. Richards in 1948 [9]. It was shown that distributed networks composed of lumped resistors and equal length or commensurate lossless transmission lines (i.e., lines of an integral multiple of a given electrical length) can be treated by methods similar to those for lumped networks by using a transformation from the complex frequency variable s to a new complex variable

$$t = \tanh \frac{ls}{c} \tag{2}$$

where l is the free-space length of the basic transmission line element, and c is the velocity of EM waves. As presented, (2) applies to TEM transmission lines, but a similar transformation may be used in the case of waveguide circuits.

The mapping of the s-plane on to the t-plane is not one to one, but is periodic, corresponding to the periodic nature of the impedance function of the distributed network. The imaginary ($j\Omega$) axis of the t-plane is related to the imaginary axis (real frequency axis) of the s-plane by the equation

$$\Omega = \tan \phi \tag{3}$$

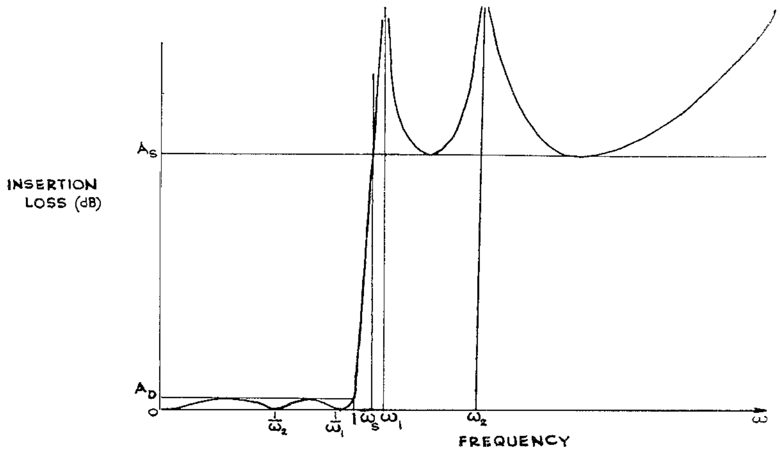

Fig. 1. Lumped-constant low-pass elliptic-function filter characteristic.

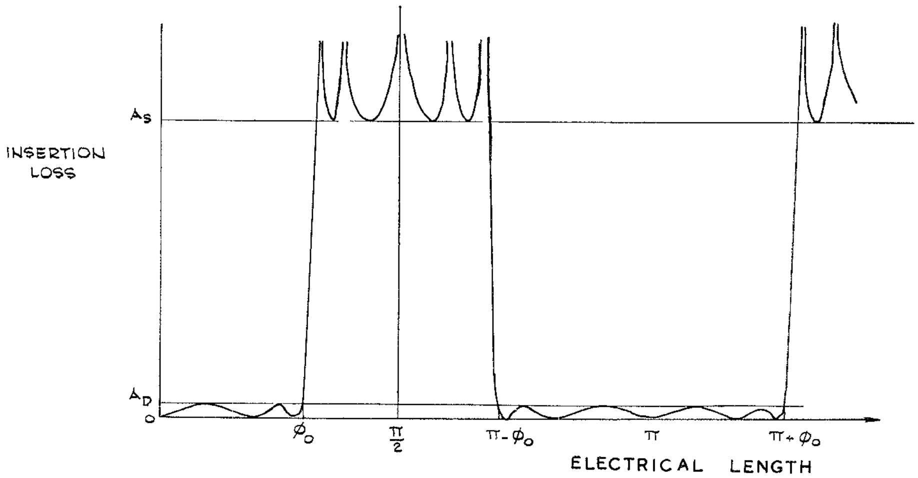

Fig. 2. Attenuation characteristic of a distributed-element elliptic-function filter.

where ϕ is the basic electrical length of the commensurate transmission lines. When the lumped network having the characteristic shown in Fig. 1 is transformed into a distributed network by Richards' transformation, the real-frequency behavior of the resulting network is shown in Fig. 2. In practice, this transformation is carried out by replacing the reactive lumped elements of the prototype by suitable transmission line stubs. Thus, an inductance of reactance $L'\omega_0$ at a frequency ω_0 is replaced by a short-circuited stub of input reactance $Z' \tan \phi_0$, and a capacitance of susceptance $C'\omega_0$ is replaced by an open-circuited stub of input susceptance $Y' \tan \phi_0$. ϕ_0 may be chosen arbitrarily, and in the example illustrated by Figs. 1 and 2 corresponds to the band edge of the low-pass filter. The choice of ϕ_0 controls the ratio of the cutoff frequencies of the second and first pass bands $(\pi-\phi_0)/\phi_0$, but too small a value of ϕ_0 may lead to extreme values for the characteristic immittances Z', Y' of the stubs.

In the transformed distributed network all the stubs are located at the same physical point, and as yet there is no provision for separation of the stubs by lengths of transmission line for ease of manufacture, and indeed, for physical realizability in the practical sense. Such a transmission line cascaded between two filter elements has the basic commensurate electrical length, and is termed a *unit element*. One of the main problems in the distributed filter design technique described in this paper is to introduce unit elements into the network without altering the insertion loss characteristic.

III. Generalized Kuroda Transformations

A method of stub separation which is used frequently in the case of certain restricted classes of ladder networks is the application of Kuroda's transformations [3], [10]. These establish an exact equivalence between a unit element in cascade with a series or shunt open- or short-circuited stub on the one hand, and the reversed cascade consisting of a stub followed by a unit element on the other. Since it is possible to incorporate any number of unit elements at either port of the ladder network, each of characteristic impedance equal to the terminating resistance at the respective ports without altering the insertion loss, then it is possible to transform these unit elements into the network by successive applications of the Kuroda transformation in such a way as to separate the stubs. This method is restrictive in that the simple Kuroda transformations apply only to single stubs,

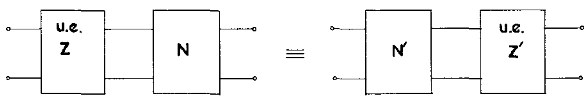

Fig. 3. Generalized Kuroda transformation.

(a) (b)

Fig. 4. Special case of a shunt Foster:

$$Z' = \frac{Z(1+LC)}{1+C(Z+L)}$$

$$C' = \frac{LC^2}{1+LC}$$

$$M = \frac{1+LC}{C}$$

$$L_p = \frac{1+C(Z+L)}{C}$$

$$L_s = \frac{(1+LC)^2}{C[1+C(Z+L)]}.$$

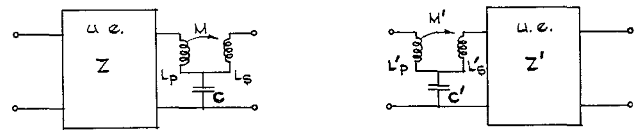

Fig. 5. The generalized Kuroda transformation applied to a Brune section:

$$Z' = \frac{Z(L_p + M^2C) + (L_p - M)^2}{L_p[1 + C(Z + L_p)]}$$

$$C' = C + \frac{1}{Z} - \frac{1}{Z'}$$

$$M'C' = MC$$

$$L_p' = \frac{ZCM^2}{Z'C'L_p}$$

$$L_s' = \frac{Z'C}{ZC'}\cdot L_p$$

$$M' - L_p' = \frac{MCZ(M - L_p - Z)}{MCZ + M - L_p}.$$

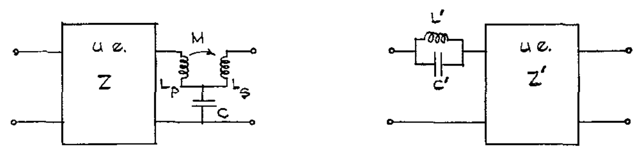

Fig. 6. Transformation of an important degenerate case for

$$Z = \frac{L_p - M}{MC}$$

$$Z' = \frac{Z}{CZ+1}$$

$$L' = \frac{Z^2C(1+MC)}{CZ+1}$$

$$L'C' = MC.$$

equivalent to a series or shunt capacitor or inductor of the lumped element prototype. However, it has now been shown [11] that the simple Kuroda transformations are special cases of a more general transformation, depicted in Fig. 3, and which may be stated as the following theorem:

> A distributed network consisting of a unit element in cascade with a physically realizable two-port may always be replaced by an equivalent circuit consisting of a physically realizable two-port in cascade with a unit element.

Thus, if the network N of Fig. 3 is defined by its transfer (or chain) matrix

$$\begin{bmatrix} A(t) & B(t) \\ C(t) & D(t) \end{bmatrix} \tag{4}$$

where t is defined in (2), then in the equivalent circuit the network N' has the transfer matrix

$$\frac{1}{1-t^2}\begin{bmatrix} A + CZt - \frac{B}{Z'}t - \frac{DZ}{Z'}t^2 & -AZ't - CZZ't^2 + B + DZt \\ C + \frac{A}{Z}t - \frac{D}{Z'}t - \frac{Bt^2}{ZZ'} & -CZ't - \frac{AZ'}{Z}t^2 + D + \frac{B}{Z}t \end{bmatrix} \tag{5}$$

and the unit element Z' is given by

$$Z' = \frac{B(1) + ZD(1)}{A(1) + ZC(1)}. \tag{6}$$

The reader is referred to the original paper [11] for the proof of (5) and (6).

In the application of this generalized transformation to elliptic-function filters, it is frequently necessary to transform a unit element across a distributed series resonant circuit in shunt (i.e., a shunt Foster), as shown in Fig. 4(a). The result of the transformation is a microwave Brune section in cascade with a unit element [5], [11], as shown in Fig. 4(b).[1] The parameters of the Brune section are given in Fig. 4, using the notation of Youla [12].

If a further transformation of a unit element is required, this will be across the microwave Brune section, which is again accomplished by means of the generalized transformation. It is easy to show that the transformation of a unit element across a Brune section results in another Brune section, as shown in Fig. 5. It is evident that this depicts a more general case than that shown in Fig. 4, where the shunt Foster of Fig. 4(a) is to be regarded as a degenerate Brune section. The equations in Fig. 4 may be derived from those of Fig. 5 by substitut-

[1] This particular transformation was first formulated by Kuroda, but published only in an internal report of a Japanese university.

ing the conditions for degeneracy, i.e., that

$$L_p = L_s = M. \tag{7}$$

In applying the generalized transformation to the Brune section the resulting Brune section is frequently degenerate, i.e., the reverse of Fig. 4 may occur. However, if the condition

$$L_p = M(CZ + 1) \tag{8}$$

occurs, then inspection of the equations in Fig. 5 shows that $C' \to 0$, while M', L_p', and $L_s' \to \infty$ in such a way that the product $M'C' = MC$. This is because the Brune section degenerates not to a shunt Foster but to a series Foster, as shown in Fig. 6, where the equations to be applied in this case are presented.

IV. Realizations of Microwave Brune Sections

A considerable amount of work on the physical realization of microwave C, Brune, and D sections has been accomplished by several workers in Japan [13], [16]. Only Brune sections are required in the realization of elliptic-function filters, since the latter has only real-frequency transmission zeros [12]. At present, no realization exists for the microwave Brune section alone, but there are several realizations for the microwave Brune section in cascade with a unit element, i.e., for the network of Fig. 4(b). The earliest such realization appears to be the Ikeno loop [13], which is shown in Fig. 7. However, this is restricted to the cases where,

$$L_s > L_p, \text{ (or } M > L_p) \tag{9}$$

$$Z > M - L_p. \tag{10}$$

Even when these conditions are satisfied, it may not be possible to construct the loop consisting of four sections of differing impedances because of impossible impedance levels.

A realization which may be more suitable than that of Ikeno was given by Saito [14], as shown in Fig. 8. Again, the impedance levels are likely to be awkward in many instances, and the restrictive conditions which apply are identical to those of the Ikeno loop, [(9), (10)].

The restrictions on the physical realization of Brune sections, as given by (9) and (10), were released to some extent by Matsumoto [14], who has given six types of realizations using three-wire lines. The formulas given by Matsumoto contain minor errors, which have been corrected by Rhodes and Scanlan [17]. In fact, it is not possible to realize a Brune section in cascade with a unit element of arbitrary impedance by a choice of one of Matsumoto's configurations. In practice it is found that some of his networks are difficult to construct, while the three-wire configuration is difficult to calculate as far as the self- and mutual-capacitance values of the wires are concerned. It has been found more convenient, therefore, to use new physical realizations as described by Rhodes, Scanlan, and Levy [18].

The first of these to be discovered was the series realization, shown in Fig. 9. The case with short-circuited stubs, Fig. 9(a), applies for $M > L_p$, and has restrictive conditons identical to those of the Ikeno loop or the Saito section. With open-circuited stubs, Fig. 9(b), cases for which $M < L_p$ may be realized, subject to a restrictive condition on Z_0 which may not be larger than $(L_p - M)/MC$. These series realizations were derived by forming the impedance matrix of the unit element/Brune section cascade, extracting the series line Z by one of two possible methods, and then synthesizing the remaining Z matrix to give the Pi network formed by Z_2, Z_3, and Z_4. It will be found that the circuits of Fig. 9 are particularly useful for filters with broad bandwidths where tight coupling of the Pi network to the series line is required. However, in cases of narrow bandwidths, the impedances Z_2 and Z_4 take extreme values. A more useful realization then is to use coupled bars and stubs,

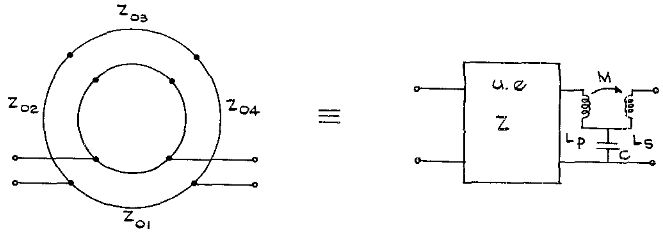

Fig. 7. Ikeno Loop. Restrictive Conditions: $M > L_p$ and $Z > M - L_p$

$$Z_{01} = \frac{(M - L_p)^2 + Z\,(L_p + M^2C)}{L_p(1 + MC)}$$

$$Z_{02} = \frac{[Z\,(M - L_p)^2 + Z\,(L_p + M^2C)]}{(M - L_p)(M - L_p + MCZ)}$$

$$Z_{03} = \frac{(M - L_p)^2 + Z\,(L_p + M^2C)}{MC(M - L_p + MCZ)}$$

$$Z_{04} = \frac{(M - L_p)^2 + Z\,(L_p + M^2C)}{L_pC(Z - M + L_p)}.$$

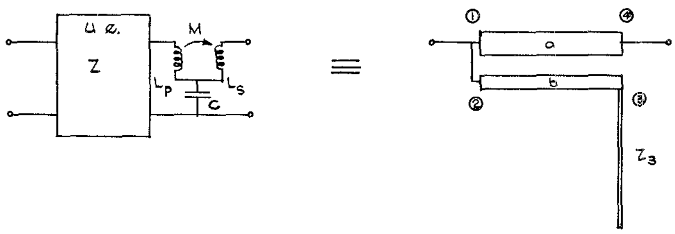

Fig. 8. Saito section. Restrictive Conditions: $M > L_p$ and $Z > M - L_p$

$$vC_a = \frac{L_p}{MZ} \qquad vC_b = \frac{M - L_p}{MZ}$$

$$vC_{ab} = \frac{L_p(Z - M + L_p)}{M^2Z} \qquad Z_3 = \frac{1}{vC}$$

where the even and odd mode impedances are given in terms of the self and mutual capacitances of the coupled bars by the equations.

$$Z_{oe}^a = \frac{C_b + 2C_{ab}}{vF} \qquad Z_{oo}^a = \frac{C_b}{vF}$$

$$Z_{oe}^b = \frac{C_a + 2C_{ab}}{vF} \qquad Z_{oo}^b = \frac{C_a}{vF}$$

$$F = \begin{vmatrix} C_a + C_{ab} & -C_{ab} \\ -C_{ab} & C_b + C_{ab} \end{vmatrix}.$$

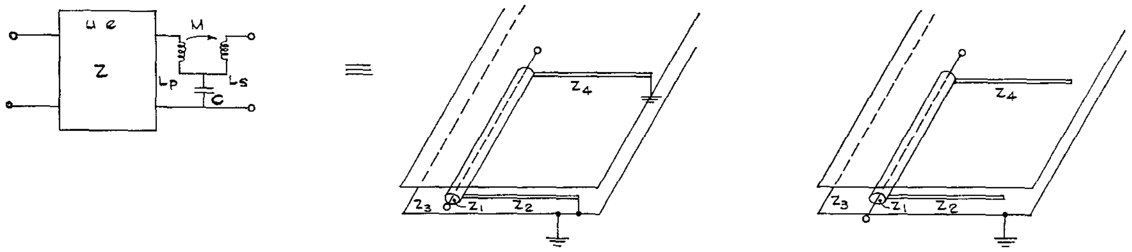

For $M > L_p$ $\quad Z > M - L_p$

$$Z_1 = \frac{Z}{(1 + Z_c)}$$

$$Z_2 = \frac{Z^2C(ZMC + M - L_p)}{(CZ + 1)^2(M - L_p)}$$

$$Z_3 = \frac{Z(ZMC + M - L_p)}{L_p(CZ + 1)}$$

$$Z_4 = \frac{Z(ZMC + M - L_p)^2}{L_p(1 + CZ)(L_p + Z + M)}$$

(a)

For $M < L_p$ $\quad Z < (L_p - M)/MC$

$$Z_1 = \frac{MZ}{L_p}$$

$$Z_2 = \frac{(L_p - M + Z)Z}{L_p}$$

$$Z_3 = \frac{(L_p - M)(L_p - M + Z)}{L_p}$$

$$Z_4 = \frac{(L_p - M)(L_p - M - MCZ)}{L_p^2C}$$

(b)

Fig. 9. Series realization of a cascade of a unit element and a Brune section.

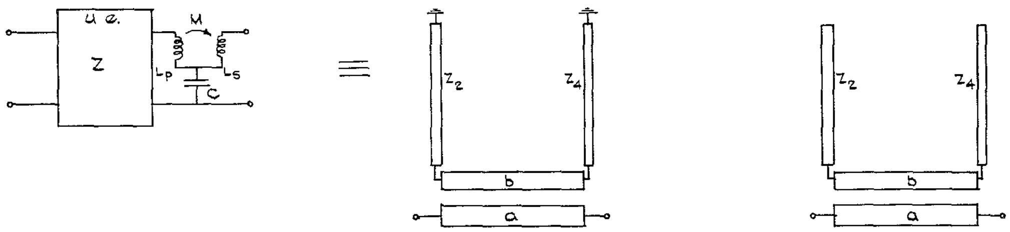

$M > L_p$. $\quad Z > M - L_p$. $\qquad$ $M < L_p$. $\quad Z < \dfrac{L_p - M}{MC}$

$$Z_b = \frac{Z_{oe}^b + Z_{oo}^b}{2}, \text{ is a parameter}$$

$$\frac{Z_{oe}^a + Z_{oo}^a}{2} = \frac{MZ}{L_p}$$

$$\frac{Z_{oe}^a - Z_{oo}^a}{2} = \frac{Z_{oe}^b - Z_{oo}^b}{2} = \sqrt{\frac{(MCZ + M - L_p)ZZ_b}{L_p(CZ + 1)}}$$

$$Z_2 = \frac{CL_pZ}{(M - L_p)(CZ + 1)}\cdot Z_b$$

$$Z_4 = \frac{(MCZ + M - L_p)}{(Z + L_p - M)(CZ + 1)}\cdot Z_b$$

(a)

$$\frac{Z_{oe}^a + Z_{oo}^a}{2} = Z + \frac{(L_p - M)^2}{L_p}$$

$$\frac{Z_{oe}^a - Z_{oo}^a}{2} = \frac{Z_{oe}^b - Z_{oe}^b}{2} = \sqrt{\frac{(L_p - M)(Z + L_p - M)Z_b}{L_p}}$$

$$Z_2 = \frac{Z}{(L_p - M)}\cdot Z_b$$

$$Z_4 = \frac{(L_p - M - MCZ)}{L_pC(L_p - M + Z)}\cdot Z_b$$

(b)

Fig. 10. Parallel-coupled line realization of a unit element/Brune section cascade.

as shown in the two circuits of Fig. 10. Originally these were derived independently by analysis, but it is readily shown that the series circuits of Fig. 9 are special cases of those of Fig. 10. Thus Fig. 9(a) is derived by making the following substitution for Z_b in Fig. 10(a):

$$Z_b = \frac{MCZ + M - L_p}{L_p(CZ + 1)} Z. \tag{11}$$

Similarly, Fig. 10(b) reduces to Fig. 9(b) with the substitution

$$Z_b = \frac{(L_p - M)(Z + L_p - M)}{L_p}. \tag{12}$$

From the restrictive conditions on Z it may appear that these coupled-line circuits are of limited use. However, in practice the restrictions are not serious, since Scanlan and Rhodes [17] have shown that, given a prescribed physically realizable driving point impedance with transmission zeros all at real frequencies, it is always possible to find a physical realization consisting of a cascade of unit elements and Brune sections satisfying these restrictions (which appear to be basic). Thus, in a synthesis procedure it may not be possible to extract a Brune section at some stages, but by first extracting one or more unit elements the eventual extraction of the Brune section for the particular transmission zero is guaranteed. In practice it is rarely necessary to extract more than one or two unit elements before the Brune section may be realized.

Examples showing how these unit element/Brune section structures are used in the design of elliptic-function microwave filters will now be given. The most important requirement is that the impedances of all lines within the filters have values which can be readily made in practice, i.e., lying in the range 10Ω to 200Ω. In this context it should be noted that physical realizability criteria in the strict circuit theory sense are not sufficient for actual practical realizations because they do not exclude structures with impossible impedance levels.

V. Examples of Elliptic-Function Microwave Filter Design Using Brune Sections

A. Band-Stop Filter from Single-Pole Prototype Having Approximately 6 Percent Bandwidth

The low-pass prototype taken from Saal's tables [2] is type number CO4 15c for a modular angle $\theta = 31°$, having a low-pass ripple level corresponding to a reflection coefficient of 0.15, and a minimum stop band attenuation of 40.2 dB, as shown in Fig. 11(a), the prototype circuit being shown in Fig. 11(b). If Richards' transformation is applied directly to a low-pass prototype, then the resulting distributed filter is of band-stop character, with the stop bands repeating at harmonic frequencies. However if a narrow stop bandwidth is required, then it has been found necessary to transform the low-pass prototype into a lumped-element band-stop filter before applying Richards' transformation. This prevents the occurrence of lines with extreme values of impedance. The characteristic of the band-stop filter is shown in Fig. 11(c), and the circuit is shown in Fig. 11(d), having applied the frequency transformation

$$\omega \rightarrow \frac{1}{\delta\left(\omega - \dfrac{1}{\omega}\right)}$$

where

$$\delta = \left| \frac{\omega_2}{\sqrt{\omega_1\omega_2}} - \frac{\sqrt{\omega_1\omega_2}}{\omega_2} \right|, \tag{13}$$

ω_1, ω_2 being the band-stop edge frequencies shown in Fig. 11(c) and, in the present instance, $\delta = 0.1$. It will be noted that the band-stop filter is a cascade of shunt and series Foster sections, i.e., of degenerate Brune sections. When Richards' transformation is applied to this lumped-element filter, taking the electrical length at the center of the stop band as $\phi_0 = 45°$, [Fig. 11(e)], it is seen that the stop bandwidth of the first harmonic stop band, defined to the pass band ripple level is slightly greater than 6 percent. It is now necessary to transform unit elements from source and load ends of the filter to give a practical realization. The fact that the filter consists of a cascade of degenerate Brune sections facilitates this process. The distributed circuit resulting when one unit element is transformed from the left-hand side and two unit elements from the right-hand side of Fig. 11(d) are shown in Fig. 11(f). The transformations depicted in Figs. 4 and 6 are used in this example. The realization in the coupled-line form with stubs is shown in Fig. 11(g), which is obtained from Fig. 11(f) using the equivalence of Fig. 10(a), and also the equivalence of Fig. 12, which is used to realize the series Foster/unit element combination at the right-hand end of the network. Note that unit elements of value $Z_0 = 1$ external to the filter at both source and load ends were used in the transformations. The normalized impedances of all stubs lie in the range 0.896 to 1.09, the impedances of the coupled lines are also approximately unity, and the coupling coefficients of the parallel-coupled line sections are easily realizable. This filter is illustrated in Fig. 13, and the measured response in Fig. 14.

Using this technique of resonating the prototype filter, stop band filters for any bandwidth from 0.1 percent or less to 100 percent may be realized (Section VII).

B. An Octave-Bandwidth Band-Pass Filter Derived From a Double-Pole Prototype

The low-pass prototype is shown in Fig. 15(a), and has the response given in Fig. 15(b). In order to form a band-pass response in the distributed case, this must be converted to a high-pass structure, and to give a bandwidth of one octave, it is necessary to arrange the cutoff frequency to occur at an electrical length $\phi_0 = 60°$. The transformation to be applied to Fig. 15(a) is thus

$$s = \frac{\tan \phi_0}{t} \tag{14}$$

which gives the pseudo high-pass circuit of Fig. 15(c) in the t-variable. The response in the distributed domain is an octave bandwidth band-pass filter with harmonics, as shown in Fig. 15(d).

A convenient way to apply the general transformation to a case of this type is to combine the three shunt inductors using the transformation shown in Fig. 16. This gives an exact equivalent of a shunt Foster in cascade with an inductance and an inductance in cascade with a Brune section. This is a degenerate case of the interchange of a Brune section with a shunt inductance, shown in Fig. 17, which may be of use in some cases. When the result of Fig. 16 is applied to the circuit of Fig. 15(c), Fig. 15(e) results. Unit elements must now be transferred into the network across the Brune sections, and the result of transferring one unit element from the left and two from the right is given in Fig. 15(f). It is necessary to transform two unit elements over the right-hand Brune section because it is not possible to realize the Brune section in cascade with a unit element at the right (having $Z = 1$) after only one transfer. The next problem is to eliminate the ideal transformer at the left, and to obtain realizable impedances. This is achieved by dividing the inductance in a suitable optimum way, and transforming the various component parts across the available unit elements. A convenient way of carrying out this process is by use of the capacitance matrix transformation described by Wenzel [19] which is simpler than the repeated application of the Kuroda identities, particularly when several unit elements are involved. One result of this process is given by the circuit of Fig. 15(g). This could be realized in practice with some difficulty; the difficulty arising because the inductance of value 0.1958 is rather low. To eliminate this

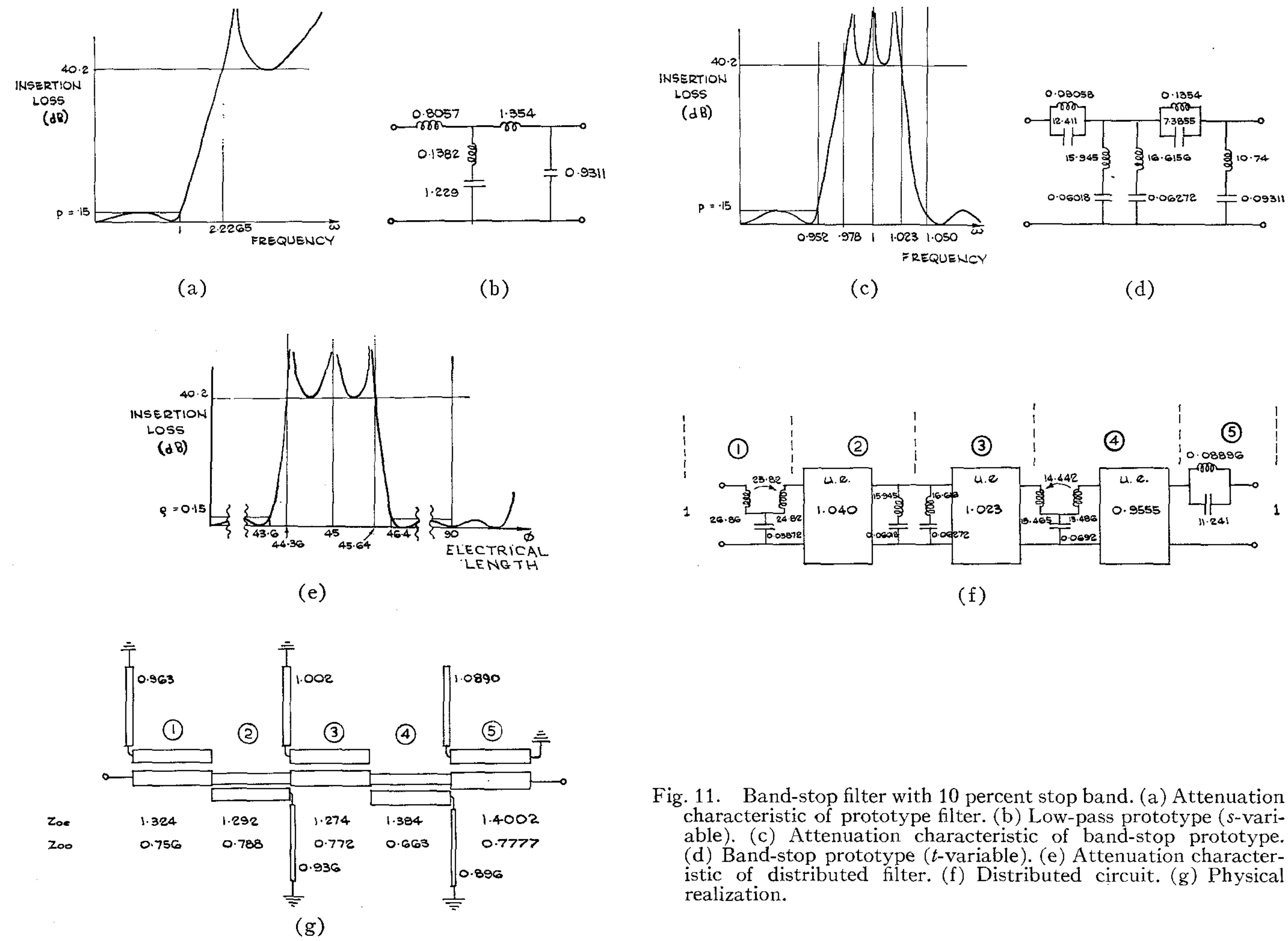

Fig. 11. Band-stop filter with 10 percent stop band. (a) Attenuation characteristic of prototype filter. (b) Low-pass prototype (s-variable). (c) Attenuation characteristic of band-stop prototype. (d) Band-stop prototype (t-variable). (e) Attenuation characteristic of distributed filter. (f) Distributed circuit. (g) Physical realization.

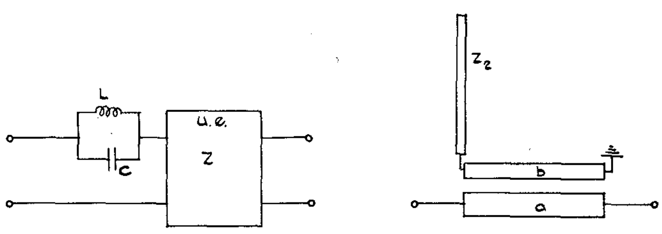

Fig. 12. Parallel-coupled line realization of a series Foster/unit element cascade.

$$Z_b = \frac{Z_{oe}{}^b + Z_{oo}{}^b}{2} \text{ is a parameter}$$

$$Z_a = \frac{Z_{oe}{}^a + Z_{oo}{}^a}{2} = Z + \frac{L^2C}{1 + LC}$$

$$\frac{Z_{oe}{}^a - Z_{oo}{}^a}{2} = \frac{Z_{oe}{}^b - Z_{oo}{}^b}{2} = \sqrt{L\left(\frac{Z}{L + Z\,(1 + LC)} + \frac{LC}{1 + LC}\right)\cdot Z_b}$$

$$Z_2 = \frac{(1 + LC)Z\,Z_b}{LC[L + Z\,(1 + LC)]}$$

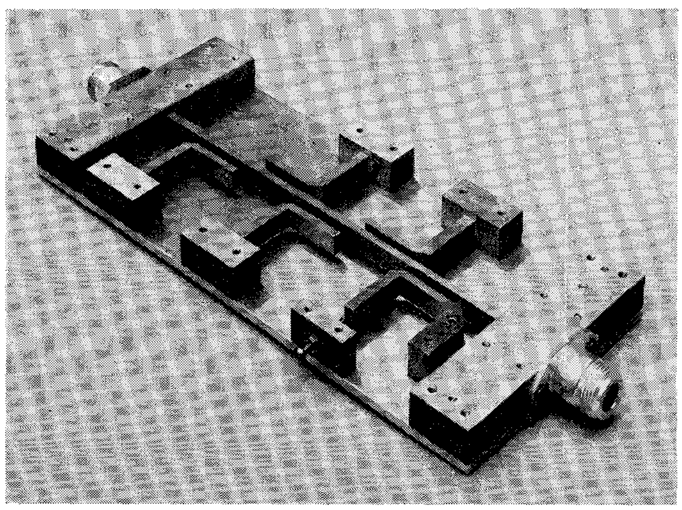

Fig. 13. Band-stop filter with one ground plane removed.

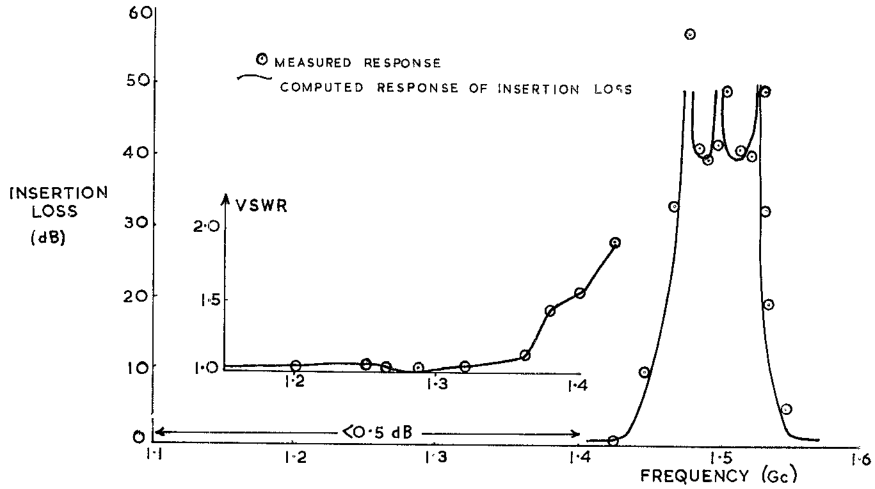

Fig. 14. Measured and computed characteristics of the band-stop filter shown in Figs. (11) and (13).

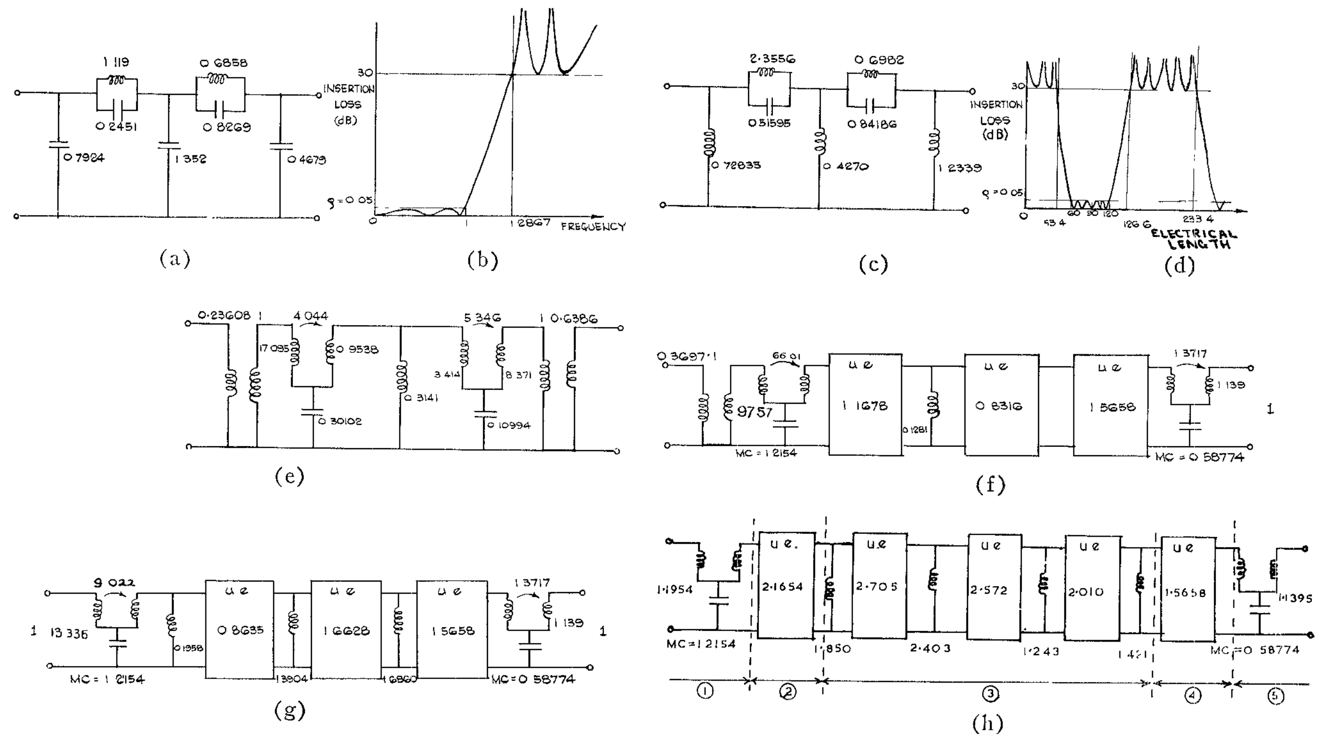

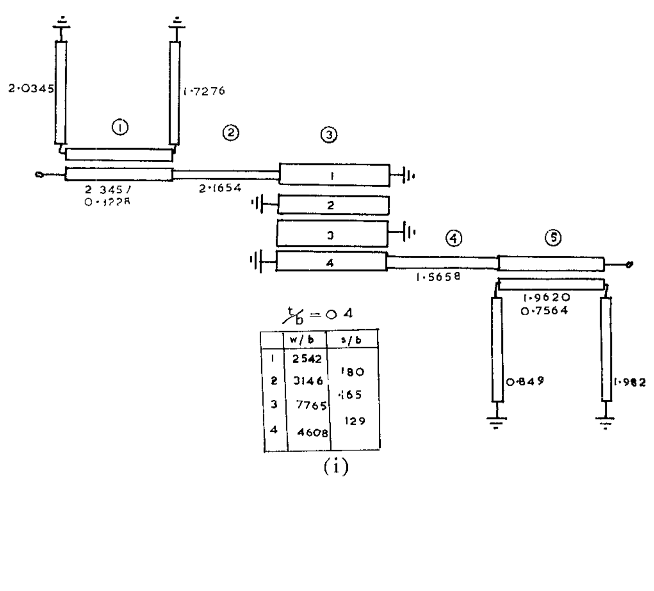

Fig. 15. Derivation of two-pole octave bandwidth filter. (a) Prototype low-pass filter (s-variable). (b) Attenuation characteristic of low-pass prototype. (c) Band-pass circuit (t-variable). (d) Attenuation characteristic of band-pass circuit. (e) Transference of inductors into center. (f) Introduction of 3 unit elements. (g) Removal of ideal transformers. (h) Introduction of two unit elements from LHS, and re-arrangement of inductors. (i) Physical realization of (h).

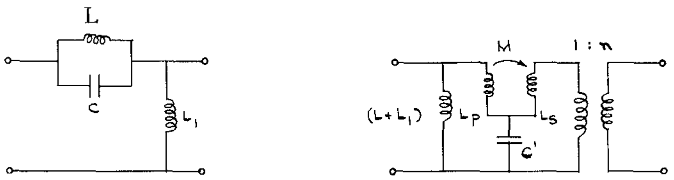

Fig. 16. Interchange of series Foster and an inductance:

$$M = \frac{(L + L_1)^2}{L}$$
$$L_p = \frac{L_1(L + L_1)}{L}$$
$$MC' = LC$$
$$n = \frac{L_1}{L + L_1}.$$

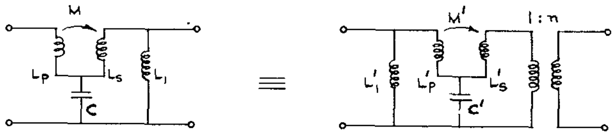

Fig. 17. Interchange of a Brune section and an inductance:

$$L_1' = L_1 + \frac{(L_p - M)^2}{L_p}$$
$$C' = \left(\frac{L_1'(L_1 + L_s)}{L_1^2} - \frac{L_p}{L_1}\right) C$$
$$M'C' = MC$$
$$n = L_1/L_1'$$
$$L_p'C' = nCL_p \qquad L_s'C' = CL_1'/n.$$

difficulty it was decided to introduce a certain degree of redundancy by transforming two additional unit elements across the left-hand Brune section. When the inductances had been redistributed the network of Fig. 15(h) resulted, which may be realized very easily as shown in Fig. 15(i). Note that the parallel-coupled line, section one, may be realized conveniently using the re-entrant line technique described by Cohn [20]. The values of ω/b and s/b for the interdigital section three are derived using Wenzel's results [19], the configuration used being rectangular coupled bars which are treated accurately by Getsinger [21].

The final configuration is somewhat bulky and inconvenient, and with further development might eventually be realized in more compact form, e.g., as an interdigital filter with stubs. Alternatively, the method of Horton and Wenzel [6], which is limited to broadband filters, would give a compact structure in the present instance.

VI. Alternative Procedure Using the Pi-Equivalent of a Brune-Section

As an alternative to the direct realization of the distributed section, it is occasionally possible to convert the Brune section into its Pi equivalent shown in Fig. 18, which consists of a series Foster and two shunt capacitors, one of the latter being negative. The negative capacitor may often be absorbed into an adjacent shunt capacitor of greater value.

As an example, a distributed pseudo low-pass filter with a stop band attenuation A_s of greater than 27.1 dB was designed. This rather low value of attenuation was chosen to simplify measurements on the filter. (A filter with $A_s > 60$ dB was also designed, and achieved the predicted rate of cutoff, but it was more difficult to establish the maxima and minima of stop band attenuation in this case.) The pass band ripple reflection coefficient was 0.20. The low-pass prototype is shown in Fig. 19(a), with the response characteristic of Fig. 19(b). The low-pass cutoff frequency for the distributed filter is shown at an electrical length $\phi_0 = 41°$, giving the characteristic shown in Fig. 19(c). Fig. 19(d) indicates the transformation of a unit element into the center of the filter, and the signs of the resulting shunt capacitors are indicated. Elimination of the negative capacitor C_2 is possible if C_1 is of greater magnitude, which is true for the prototype and cutoff electrical length ϕ_0 chosen. (It is usually true if the value of ϕ_0 is chosen to be near 45°). This process is repeated until five unit elements have been transformed, giving the circuit of Fig. 19(e). Note that the admittance of the first shunt stub is extremely low and, in practice, may be disregarded.

The physical realization using slab-line [22] is shown in Fig. 20, where the shunt Fosters are realized directly using the equivalence given in Fig. 21. The comparison between theory and experiment is shown in Fig. 22. No attempt was made to allow for fringing capacitances at the ends of the open-circuit stubs and no tuning was attempted, so that the results may be considered quite encouraging.

VII. Bandwidth Limitations of the Various Filter Designs

Investigations of the range of bandwidths which result in realizable filter designs have been carried out for some cases using a computer, and the results are presented in Table I. This shows that band-stop filters of the single-pole type are realizable over a wide range, and double-pole filters over a more restricted range of bandwidths. Note that Table I does not present a complete picture even for these cases since it considers only particular forms of realization, i.e., with only the coupled bar type of unit element/Brune sections, and with a specified number of unit elements. By considering other Brune section realizations and by introduction of further unit elements, it is often possible to extend the range of realizable bandwidths. In fact, it would be difficult to present a complete picture because of the large number of circuits which exist.

Results are not yet available for band-pass filters of the type presented in Section V-B. However, it appears that the method described in that section, i.e., using an unresonated prototype, is suitable only for broadband filters for which, as stated previously, the method of Horton and Wenzel [6] is possibly more appropriate. It is expected that filters based on a resonated prototype would be realizable for narrow bandwidths as in the case of band-stop filters.

The double-pole resonated band-stop filter design of Table I, i.e., case (b), requires application of an approximation to a nearly degenerate Brune section. This

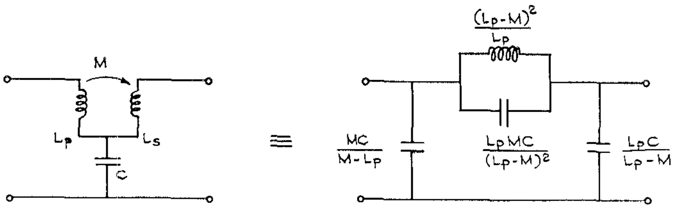

Fig. 18. Pi equivalent of a Brune section.

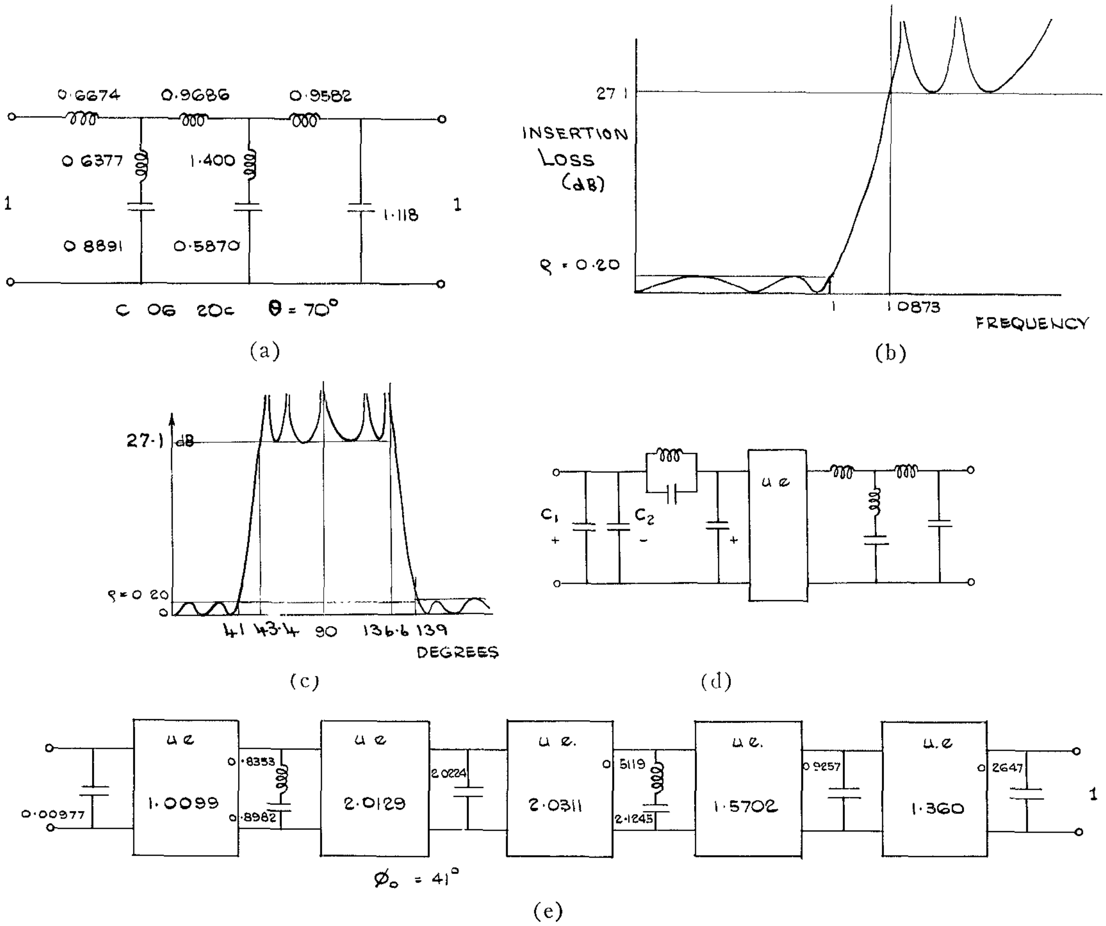

Fig. 19. Derivation of low-pass filter without Brune sections. (a) Low-pass prototype. (b) Attenuation characteristic of low-pass prototype (c) Attenuation characteristic of distributed circuit. (d) Transformation of one unit element. (e) Transformation of five unit elements.

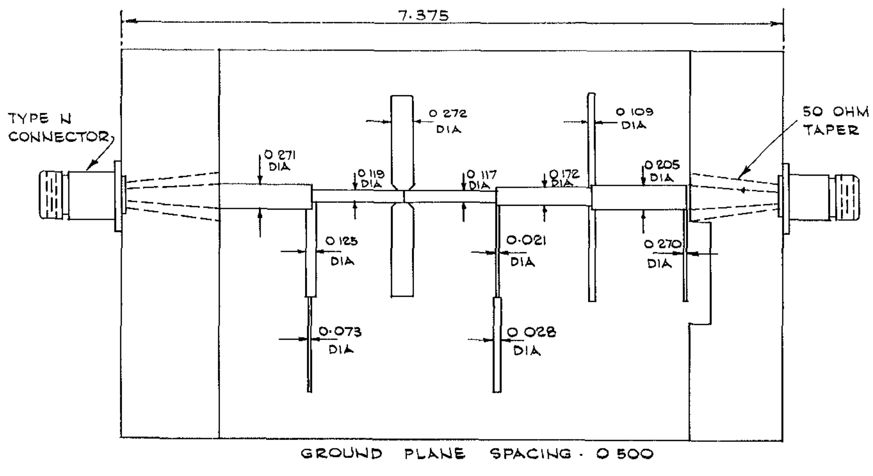

Fig. 20. Sketch of slab-line realization of Fig. 19(c)

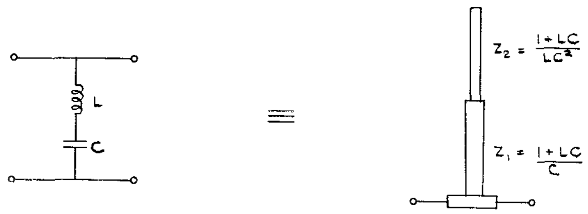

Fig. 21. Equivalence of a distributed shunt Foster.

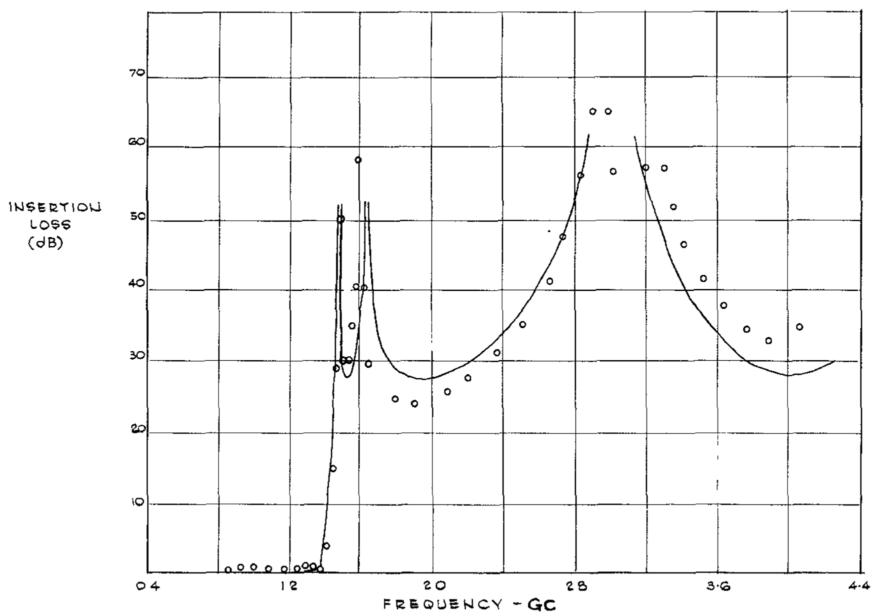

Fig. 22. Measured and computed attenuation characteristic of filter of Fig. 20.

TABLE I

Realizable Band-Stop Filters With Coupled-Bar Type Brune Sections (Fig. 10)

Type	Stop-band attenuation level, A_s (dB)	Pass-band reflection coefficient, ρ	Approximations required	Range of impedances occurring within the filter (Ω)	Range of bandwidths realizable
(a) Single-pole resonated prototype band-stop. See Fig. 11.	30–75	0.01–0.25	None	12–150	0–100%
(b) Double-pole resonated prototype band-stop—similar to Fig. 11 but having seven sections in cascade.	75	0.01	Nearly-degenerate Brune sections with one very low impedance stub occur, and are approximated by degenerate sections as described in the text.	Always approximately 50 Ω	0–15%
	30	0.01			0–5%
	60	0.15			0–6%
	30	0.15			0–4%

applies when (8) is very nearly satisfied, i.e., when $(L_p - M - MCZ_0)$ is positive but near zero. The stub impedance Z_4 of Fig. 10(b) is then very low, so that the Brune section is nearly degenerate and may be approximated by the realization shown in Fig. 12. In the exact Brune section M, L_p, and L_s are large and have values which are approximately equal, and C is small. MC has a value close to unity, i.e.,

$$MC \simeq L_pC \simeq L_sC \simeq 1. \tag{15}$$

The transfer matrix of a Brune section is

$$\frac{1}{1 + MCt^2}\begin{bmatrix} 1 + L_pCt^2 & \dfrac{(L_p - M)^2}{L_p}t \\ Ct & 1 + L_sCt^2 \end{bmatrix}. \tag{16}$$

In the nearly degenerate case this may be well-approximated by the matrix

$$\frac{1}{1 + L'C't^2}\begin{bmatrix} 1 + L'C't^2 & L't \\ 0 & 1 + L'C't^2 \end{bmatrix} \tag{17}$$

where

$$L' = \frac{(L_p - M)^2}{L_p} \qquad L'C' = MC \tag{18}$$

giving a transmission zero at the same frequency. Matrix (17) is realized by the degenerate Brune section of Fig. 12.

VIII. Conclusions

Previously, most designs for microwave filters have been based on Butterworth or Chebyshev insertion loss functions. It has been shown how to design microwave filters with elliptic-function response, which has an advantage of giving poles of attenuation near the cutoff frequencies, and hence faster rates of cutoff than Chebyshev filters of equal degree and equal band-pass insertion loss. The design procedure commences from a lumped-constant prototype filter for which comprehensive tables of element values have been previously published [2]. This is standard practice in many existing microwave filter design methods. A generalization of the well-known Kuroda's identities is used to introduce unit elements (lengths of transmission-line in cascade) into the filter in order to separate the various stubs and other elements of the filter.

In general, it is found that distributed forms of the Brune section are required in order to realize the filters, and several such realizations have been presented. It has been shown that practical configurations result for both narrow and broadband filters of pseudo low-pass or pseudo high-pass character.

Reasonably good agreement with theory has been obtained for practical filters. In addition to the special case of elliptic function types, the method would be applicable to general filter characteristics.

Acknowledgment

The authors are grateful to J. O. Scanlan and J. D. Rhodes for valuable discussions in the course of this work.

References

[1] S. Darlington, "Synthesis of reactance 4-poles which produce prescribed insertion loss characteristics," *J. Math. Phys.*, vol. 18, pp. 257–353, September 1939.
[2] R. Saal, *Der Entwurf von filtern mit Hikfe des Kataloges Normierter Tiefpässe.* Backnang/Würtemberg, W. Germany: Telefunken, G.M.B.H.
[3] H. Ozaki and J. Ishii, "Synthesis of transmission-line networks and the design of UHF filters," *IRE Trans. on Circuit Theory*, vol. CT-2, pp. 325–336, December 1955.
[4] N. Saito, "Coupled transmission-line filter," *Sci. Repts. Res. Insts. Tohoku Univ.*, Sendai, Japan, Ser. B-(Elec. Comm.), vol. 14, no. 1, pp. 9–19, 1962.
[5] M Blanc and M. Soldi, "Nota sul calcolo di filtri con parametri distribuiti," *Alta Frequenza*, vol. 32, pp. 649–657, September 1963.
[6] M. C. Horton and R. J. Wenzel, "Realization of microwave filters with equal ripple response in both pass and stop bands," presented at the 1966 Internat'l Symp. on Generalized Networks, Polytechnic Institute of Brooklyn, Brooklyn, N. Y.
[7] B. M. Schiffman, "A multiharmonic rejection filter designed by an exact method," *IEEE Trans. on Microwave Theory and Techniques*, vol. MTT-12, pp. 512–516, September 1964.
[8] E. N. Torgow and P. D. Lubell, "Band-pass filters with steep skirt selectivity," *IEEE Trans. on Microwave Theory and Techniques*, vol. MTT-13, pp. 124–126, January 1965.
[9] P. I. Richards, "Resistor-transmission-line circuits," *Proc. IRE*, vol. 36, pp. 217–220, February 1948.
[10] H. Ozaki and J. Ishii, "Synthesis of a class of strip-line filters," *IRE Trans. on Circuit Theory*, vol. CT-5, pp. 104–109, June 1958.
[11] R. Levy, "A general equivalent circuit transformation for distributed networks," *IEEE Trans. on Circuit Theory* (*Correspondence*), vol. CT-12, pp. 457–458, September 1965.
[12] D. C. Youla, "A new theory of cascade synthesis," *IRE Trans. on Circuit Theory*, vol. CT-9, pp. 244–260, September 1961.
[13] H. Ozaki and J. Ishii, "On the design of distributed constant networks," *IEEE Trans. on Circuit Theory* (*Reviews of Current Literature*), vol. CT-4, pp. 22–23, March 1957.
[14] *Network Synthesis With Multiwire Lines*, A. Matsumoto, Ed., Monograph series, Research Institute of Applied Electricity, Hokkaido University, Sapporo, Japan, no. 11, 1963.
[15] *Developments in Multiwire Networks*, A. Matsumoto, Ed., Monograph series, Research Institute of Applied Electricity, Hokkaido University, Sapporo, Japan, no. 12, 1964.
[16] G. I. Zysman and A. Matsumoto, "Properties of microwave C-sections," *IEEE Trans. on Circuit Theory*, vol. CT-12, pp. 74–82, March 1965.
[17] J. O. Scanlan and J. D. Rhodes, "Cascade synthesis of distributed networks," presented at the 1966 Internat'l Symp. on Generalized Networks, Polytechnic Institute of Brooklyn, Brooklyn, N. Y.
[18] J. D. Rhodes, J. O. Scanlan and R. Levy, "Realization of microwave Brune sections," *Elec. Lett.*, vol. 1, pp. 268–269, November 1965.
[19] R. J. Wenzel, "Exact theory of interdigital band-pass filters and related coupled structures," *IEEE Trans. on Microwave Theory and Techniques*, vol. MTT-13, pp. 559–575, September 1965.
[20] S. B. Cohn, "The re-entrant cross-section and wide-band 3 db hybrid couplers," *IEEE Trans. on Microwave Theory and Techniques*, vol. MTT-11, pp. 254–258, July 1963.
[21] W. J. Getsinger, "Coupled rectangular bars between parallel plates," *IRE Trans. on Microwave Theory and Techniques*, vol. MTT-10, pp. 65–72, January 1962.
[22] R. M. Chisholm, "The characteristic impedance of trough and slab lines," *IRE Trans. on Microwave Theory and Techniques*, vol. MTT-4, pp. 166–172, July 1956.